Asian Journal of Chemistry; Vol. 34, No. 3 (2022), 569-574

ASIAN JOURNAL OF CHEMISTRY

https://doi.org/10.14233/ajchem.2022.23492

Boron Nitride Reinforced Flexible Poly(L-lactide)-*b*-polyethylene glycol-*b*-poly(L-lactide) Bioplastic: Evaluation of Thermal, Morphological and Mechanical Properties

THEERAPHOL PHROMSOPHA and YODTHONG BAIMARK*

Biodegradable Polymers Research Unit, Department of Chemistry and Center of Excellence for Innovation in Chemistry, Faculty of Science, Mahasarakham University, Mahasarakham 44150, Thailand

*Corresponding author: Tel./Fax: +66 43 754246; E-mail: yodthong.b@msu.ac.th

Received: 21 August 2021; *Accepted*: 30 October 2021; *Published online*: 14 February 2022; AJC-20687

Poly(L-lactide)-*b*-polyethylene glycol-*b*-poly(L-lactide) triblock copolymer (PLLA-PEG-PLLA)/exfoliated boron nitride (BN) composite films with different boron nitride contents (1, 2, 4 and 6 wt.%) were prepared by a solution-suspension casting method. Differential scanning calorimetry (DSC), thermogravimetric analysis (TGA), scanning electron microscopy (SEM), X-ray diffractrometry (XRD) and tensile testing were carried out to characterize the thermal, morphological and mechanical properties of composite films. The DSC and XRD analyses showed the increasing crystallinity-content of composite films was obtained and their thermal stability as assessed by thermogravimetric analysis was improved when the boron nitride content was increased until 2 wt.%. Aggregation of boron nitride particles in composite films occurred when the boron nitride contents were higher than 2 wt.% as observed from SEM. The tensile stress of PLLA-PEG-PLLA film (25.0 MPa) increased up to 31.6 MPa while strain at break decreased from 76% to 64% when the 2 wt.% boron nitride was blended. Thus, PLLA-PEG-PLLA/BN composite films have potential to be used as flexible bioplastics.

Keywords: Poly(lactic acid), Block copolymer, Boron nitride, Polymer composites, Mechanical properties.

INTRODUCTION

Poly(L-lactic acid) or poly(L-lactide) (PLLA) is a potential bioplastic to replace petroleum-based plastics because of its non-toxicity, biodegradability, bio-renewability, high mechanical strength and good processability [1-3]. PLLA has been used in several industrial applications such as biomedical, pharmaceutical, automotive interiors and packaging [4-6]. However, slow crystallization and low flexibility have been found to be significant problems limiting the practical use of PLLA [1,7,8]. PLLA-*b*-polyethylene glycol-*b*-PLLA triblock copolymers (PLLA-PEG-PLLA) were found to be more flexible than PLLA because their PEG middle-blocks acted as plasticizing sites to enhance chain mobility of the PLLA end-blocks [9-11]. However, PLLA-PEG-PLLA has lower mechanical strength than PLLA [10].

Various reinforcing fillers such as natural fibers [12], nanoclay [13], cellulose nanocrystals [14] and boron nitride (BN) [15] have been used to improve mechanical strength of PLLA. Among these fillers, boron nitride powder is one of the most interesting reinforcing fillers because of its good thermal and chemical stability, low reactivity and high mechanical-strength [16,17]. Moreover, boron nitride powder enhanced crystallization of PLLA [17] and poly(3-hydroxybutyrate) (PHB) [18] by acting as a heterogeneous nucleating agent.

To the best of our knowledge, there have not been any reports on the effect of boron nitride on properties of PLLA-PEG-PLLA. In this study, we aimed to improve the crystallization and mechanical strength of PLLA-PEG-PLLA by addition of boron nitride.

EXPERIMENTAL

PLLA-PEG-PLLA was synthesized through ring-opening polymerization of L-lactide monomer using stannous octoate and PEG (molecular weight of 20,000 g/mol) as the initiating system as described earlier [10,11]. Number-average molecular weight (M_n) and dispersity of this PLLA-PEG-PLLA were 89,900 g/mol and 2.8, respectively. Boron nitride powder with an average particle size of 1 μm was obtained from Qinghe Chuangya Welding Material Co., Ltd. (China). Boron nitride (1 g) was exfoliated in 40 mL of ethanol and ultrasonicated

This is an open access journal, and articles are distributed under the terms of the Attribution 4.0 International (CC BY 4.0) License. This license lets others distribute, remix, tweak, and build upon your work, even commercially, as long as they credit the author for the original creation. You must give appropriate credit, provide a link to the license, and indicate if changes were made.

for 4 h [19]. The resulting dispersions were centrifuged at 4,000 rpm for 10 min to remove non-exfoliated boron nitride particles. The supernatants were centrifuged at 9,000 rpm for 30 min to collect the exfoliated boron nitride particles before washing with deionized water and drying in an oven at 60 ºC for 24 h. The morphology of exfoliated boron nitride particles is shown in Fig. 1.

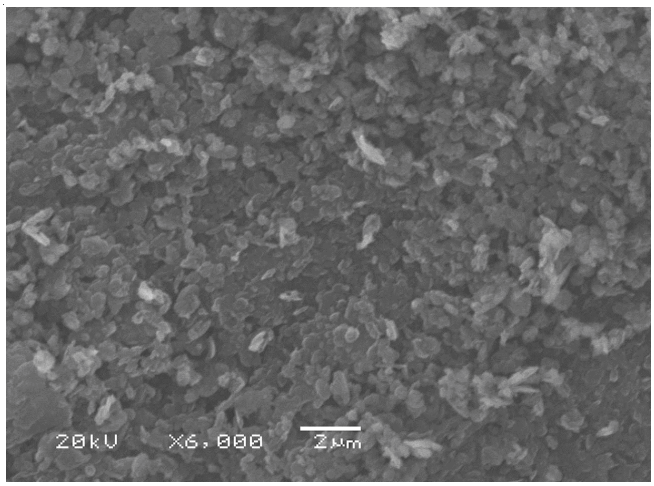

Fig. 1. SEM images of exfoliated BN particles (Bar scale = 2 μm)

Preparation of PLLA-PEG-PLLA/BN films: PLLA-PEG-PLLA/BN composite films were prepared using a solution suspension casting method. PLLA-PEG-PLLA and exfoliated boron nitride were dried under vacuum at 40 ºC overnight before mixing. The composite films with boron nitride contents of 1, 2, 4 and 6 wt.% were investigated. The boron nitride suspension was prepared by dispersion of exfoliated boron nitride in $CHCl_3$ using an ultrasonicator for 30 min before mixing with PLLA-PEG-PLLA solution in $CHCl_3$ by magnetic stirring for another 30 min. The solution-suspensions were cast on glass plates and left for solvent to evaporate at room temperature for 2 days, and then further dried under vacuum at 40 ºC until a constant weight was reached.

Characterization: Thermal transition properties of the composite films were determined using a differential scanning calorimeter (DSC, Perkin-Elmer Pyris Diamond) under nitrogen gas flow. The composite films were first heated at 200 ºC for 3 min to remove thermal history, then fast quenched before heating from 0 to 200 ºC at a rate of 10 ºC/min to observe glass transition (T_g), cold crystallization (T_{cc}) and melting (T_m) temperatures as well as enthalpies of melting (ΔH_m) and cold crystallization (ΔH_{cc}). The degree of crystallinity from DSC (DSC-X_c) of the PLLA phases was calculated from eqn. 1:

$$\text{DSC-}X_c(\%) = \frac{(\Delta H_m - \Delta H_{cc})}{(93 \times W_{PLLA})} \times 100 \quad (1)$$

where 93 J/g is the ΔH_m for 100%X_c PLLA [20]. W_{PLLA} is the PLLA weight-fraction of the composite films calculated from PLLA fraction (PLLA-PEG-PLLA = 0.83 obtained from ^{1}H NMR) [10] and the boron nitride content.

For half crystallization-time ($t_{1/2}$) determination, the composite films were first heated at 200 ºC for 3 min to completely erase thermal history, then quenched to 120 ºC at a rate of 50 ºC/min and then isothermally scanned at 120 ºC until the completion of crystallization [21]. The $t_{1/2}$ is the time required to achieve half of the final crystallinity.

Thermal stability of the composite films was determined using a thermogravimetric analyzer (TGA, TA-Instrument SDT Q600). TGA was carried out in the range of 50 to 1,000 ºC at a heating rate of 20 ºC/min under a nitrogen gas flow. Crystalline structures of the composite films were investigated using a wide-angle X-ray diffractometer (XRD, Bruker D8 Advance) in the angle range of 2θ = 5º-30º equipped with a copper tube operating at 40 kV and 40 mA producing Cu*K*α radiation. Scan speed was 3º/min. The degree of crystallinity from XRD (XRD-X_c) of the composite films was calculated from eqn. 2.

$$\text{XRD-}X_c(\%) = \frac{A_c}{(A_c + A_a)} \times 100 \quad (2)$$

where A_c and A_a are the areas of crystalline XRD peaks and amorphous halo, respectively.

Phase morphology of the composite films was observed using a scanning electron microscope (SEM, JEOL JSM-6460-LV). The composite films were cryogenically fractured after immersing in liquid nitrogen and were sputter coated with gold to avoid charging before scanning at an acceleration voltage of 15 kV. The tensile properties of the composite films were measured using an universal mechanical testing machine (Liyi Environmental Technology LY-1066B) with a load cell of 100 kg, a crosshead speed of 50 mm/min and a gauge length of 50 mm. The film sizes were 100 mm × 10 mm. The averaged tensile properties were obtained from at least five measurements.

RESULTS AND DISCUSSION

Thermal transition properties: Fig. 2 shows the DSC curves of pure PLLA-PEG-PLLA and composite films. The DSC results are summarized in Table-1. The T_g of PLLA-PEG-PLLA/BN composite films was in the range 28-30 ºC, indicating that the addition of boron nitride did not significantly change T_g values. Boron nitride addition caused shifting of T_{cc} peaks of the PLLA-PEG-PLLA matrix to lower temperature. This may be explained by boron nitride acting as a heterogeneous nucleating agent for crystallization of PLLA blocks. Boron nitride enhanced crystallization of PLLA has been reported in the literature [15]. Therefore, the DSC-X_c of composite films also increased as the boron nitride content increased. However, the T_{cc} peaks of composite films shifted to higher temperature and DSC-X_c of composite films decreased as the boron nitride contents became higher than 2 wt.% indicated that crystallization of PLLA was suppressed [22]. This may be due to aggregation of boron nitride at higher content in the composites [15]. The T_m peaks of composite films did not change with the boron nitride content.

The DSC cooling scans were carried out to determine crystallization of film samples as presented in Fig. 3 to show their T_c peaks and ΔH_c as summarized in Table-2. The T_c peak of PLLA-PEG-PLLA (107 ºC) dramatically shifted to higher temperature as boron nitride was added (114 and 115 ºC for 1 and 2 wt.% boron nitride, respectively). While the ΔH_c values

TABLE-1
DSC RESULTS OF PLLA-PEG-PLLA/BN FILMS FROM DSC HEATING SCANS

BN content (wt%)	W_{PLLA}	T_g (°C)	T_{cc} (°C)	ΔH_{cc} (J/g)	T_m (°C)	ΔH_m (J/g)	DSC-X_c (%)
–	0.830	30	75	15.4	166	37.8	29.0
1	0.8217	30	68	6.8	165	37.4	40.0
2	0.8134	29	67	5.5	165	37.0	41.6
4	0.7968	28	70	12.0	166	37.6	34.5
6	0.7802	29	73	12.4	168	37.1	34.0

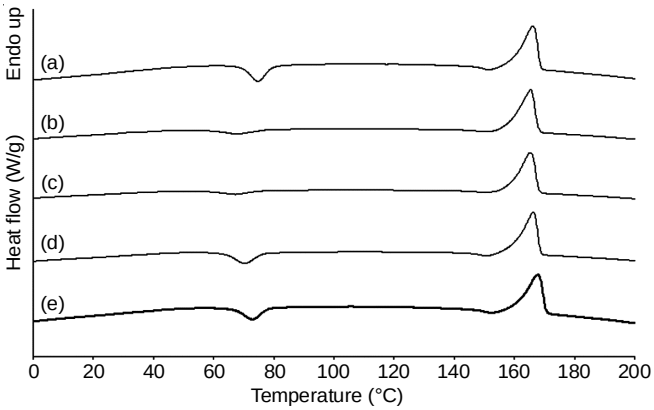

Fig. 2. DSC heating curves of (a) pure PLLA-PEG-PLLA film and PLLA-PEG-PLLA/BN films with BN contents of (b) 1, (c) 2, (d) 4 and (e) 6 wt%

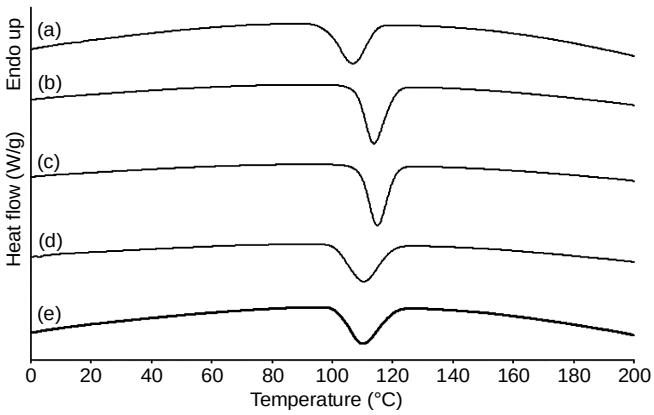

Fig. 3. DSC cooling curves of (a) pure PLLA-PEG-PLLA film and PLLA-PEG-PLLA/BN films with BN contents of (b) 1, (c) 2, (d) 4 and (e) 6 wt%

TABLE-2
DSC RESULTS OF PLLA-PEG-PLLA/BN FILMS FROM DSC COOLING AND ISOTHERMAL SCANS

BN content (wt%)	T_c (°C)[a]	ΔH_{cc} (J/g)[a]	$t_{1/2}$ (min)[b]
–	107	31.7	2.30
1	114	34.6	1.07
2	115	35.8	0.88
4	110	32.4	1.92
6	110	31.6	2.22

[a]Obtained from DSC cooling scans; [b]Obtained from DSC isothermal scans.

slightly increased with increasing the boron nitride content up to 2 wt.%. The higher temperature T_c peak and larger ΔH_c value were attributed to easier crystallization of PLLA [23]. However, the T_c peaks shifted to lower temperature and ΔH_c decreased as the boron nitride contents were raised to more than 2 wt.%.

The isothermal crystallization at 120 ºC of pure PLLA-PEG-PLLA and composite films was investigated from DSC exothermic curves as presented in Fig. 4. The $t_{1/2}$ values are also listed in Table-2, where it is seen that they decreased from 2.30 min to 1.07 min and 0.88 min when boron nitride contents were 1 and 2 wt.%, respectively. Whereas the $t_{1/2}$ values increased to 1.92 min and 2.22 min when the boron nitride contents were 4 and 6 wt.%, respectively. The results from DSC cooling and isothermal scans confirmed that the addition of 1 and 2 wt.% boron nitride can improve crystallization of PLLA blocks in PLLA-PEG-PLLA.

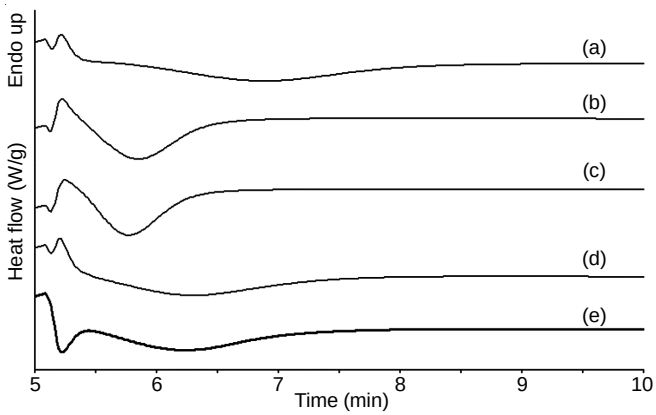

Fig. 4. DSC exothermic curves at the isothermal crystallization temperature of 120 °C of (a) pure PLLA-PEG-PLLA film and PLLA-PEG-PLLA/BN films with BN contents of (b) 1, (c) 2, (d) 4 and (e) 6 wt%

Thermal Stability: The thermal stability of pure PLLA-PEG-PLLA and composite films was determined from thermogravimetric (TG) and derivative TG (DTG) thermograms as shown in Fig. 5. The results from TG and DTG thermograms are summarized in Table-3. The TG curve of pure PLLA-PEG-PLLA is shown in Fig. 5 (above, black line) indicating that it had two thermal-decomposition steps in the ranges 250-350 ºC and 350-450 ºC attributed to thermal decompositions for PLLA and PEG blocks, respectively [10]. All composite films exhibited two thermal-decomposition steps similar to the pure PLLA-PEG-PLLA film.

Decomposition temperatures for 50% weight remaining (50%-T_d) from TG thermograms of the pure PLLA-PEG-PLLA (326 ºC) shifted to 329 ºC and 336 ºC when 1 and 2 wt.% boron nitride were added, respectively. However, the 50%-T_d values decreased to 326 ºC and 327 ºC, when boron nitride contents were 3 and 4 wt.%, respectively. The remaining weights at 1000 ºC of composite films increased with the boron nitride contents as boron nitride cannot be degraded at high temperature [15].

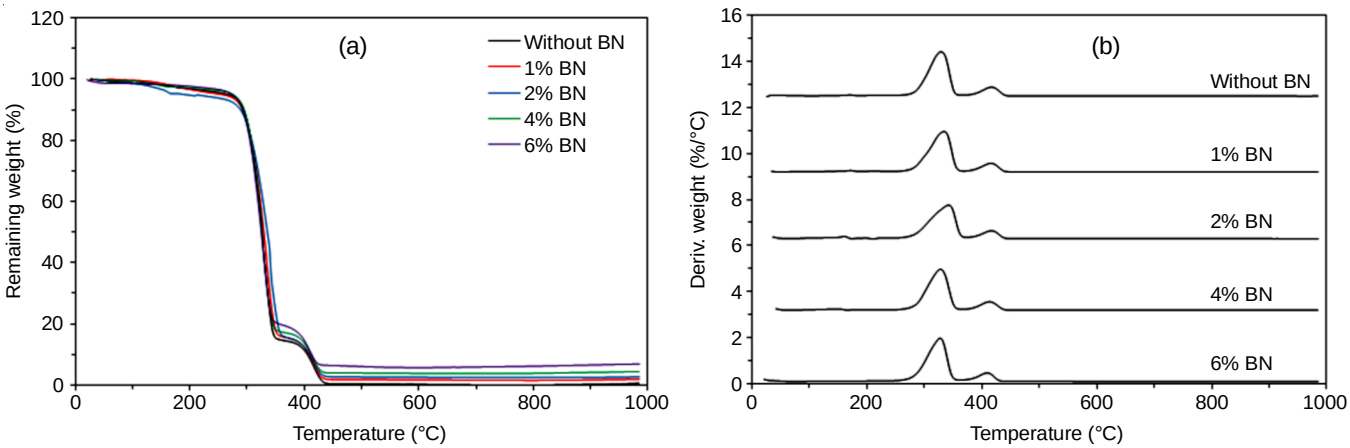

Fig. 5. TG (a) and DTG (b) thermogram curves of PLLA-PEG-PLLA/BN films with various BN contents

TABLE-3
THERMAL STABILITY OF PLLA-PEG-PLLA/BN FILMS

BN content (wt%)	50%-T_d (°C)	Remaining weight at 1,000 °C (%)	PLLA-$T_{d,max}$ (°C)	PEG-$T_{d,max}$ (°C)
–	326	0.58	328	416
1	329	1.93	336	416
2	336	2.71	342	416
4	327	4.43	329	412
6	326	6.88	329	411

Thermal stability of the composite films was confirmed from DTG thermograms as shown in Fig. 5. The peaks from DTG thermogram curves were temperatures of maximum decomposition rate ($T_{d,max}$) which are also reported in Table-3. The pure PLLA-PEG-PLLA film exhibited two $T_{d,max}$ peaks at 328 ºC and 416 ºC assigned to thermal decomposition of PLLA blocks (PLLA-$T_{d,max}$) and PEG blocks (PEG-$T_{d,max}$), respectively. The PLLA-$T_{d,max}$ of composite films significantly shifted to higher temperature as the boron nitride contents was increased. The thermal stability of composite films was improved by boron nitride, which may act as a barrier for molecular migration [24]. However, the PLLA-$T_{d,max}$ decreased when the boron nitride content was higher than 2 wt.%. This may be due to aggregation of boron nitride particles for higher content [15].

Crystalline structure: The crystalline structures of pure PLLA-PEG-PLLA and composite films were determined from XRD patterns (Fig. 6). The pure PLLA-PEG-PLLA and all the composite films had XRD peaks at 2θ = 15º, 17º and 19º attributable to the crystallites of PLLA blocks [10,11]. The XRD peak of boron nitride crystallites was found at 2θ = 27º for all the composite films [25]. Peak intensity of BN at 2θ = 27º steadily increased as the boron nitride content increased indicating that the composite films with various boron nitride contents were successfully prepared.

The XRD-X_c values of film samples are reported in Table-4 that the XRD-X_c values significantly increased as boron nitride contents increased up to 2 wt.%. When the boron nitride content was higher than 2 wt.%, the XRD-X_c values significantly decreased corresponding to the results of DSC-X_c as described above.

Film morphology: Fig. 7 shows SEM images of film cross-sections to investigate distribution and dispersion of boron

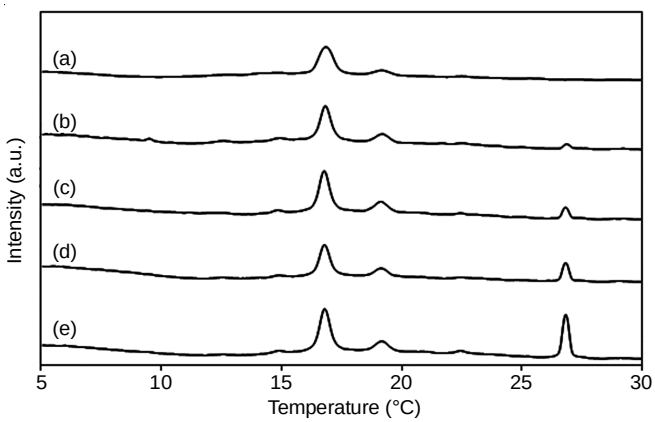

Fig. 6. XRD patterns of (a) pure PLLA-PEG-PLLA film and PLLA-PEG-PLLA/BN films with BN contents of (b) 1, (c) 2, (d) 4 and (e) 6 wt%

TABLE-4
XRD-X_c OF PLLA-PEG-PLLA/BN FILMS

BN content (wt%)	XRD-X_c (%)
–	41.1
1	43.5
2	52.5
4	48.3
6	42.1

nitride particles in the PLLA-PEG-PLLA matrix. It can be seen that the number of boron nitride particles increased with the boron nitride content. Good distribution and dispersion of the boron nitride particles were found for both the composite films containing 1 and 2 wt.% boron nitride as shown in Figs. 7b and 7c, respectively. This suggests that boron nitride particles were thoroughly compatible with PLLA-PEG-PLLA. Aggregation of boron nitride particles was clearly observed for the composite films containing 3 and 4 wt.% boron nitride as shown in Figs. 7d and 7e, respectively. These composite films exhibited good distribution but poor dispersion of boron nitride particles in the PLLA-PEG-PLLA matrix.

Tensile properties: Fig. 8 presents typical tensile curves of pure PLLA-PEG-PLLA and composite films. The averaged tensile properties are summarized in Table-5. The ultimate tensile stress and Young's modulus of the composite films

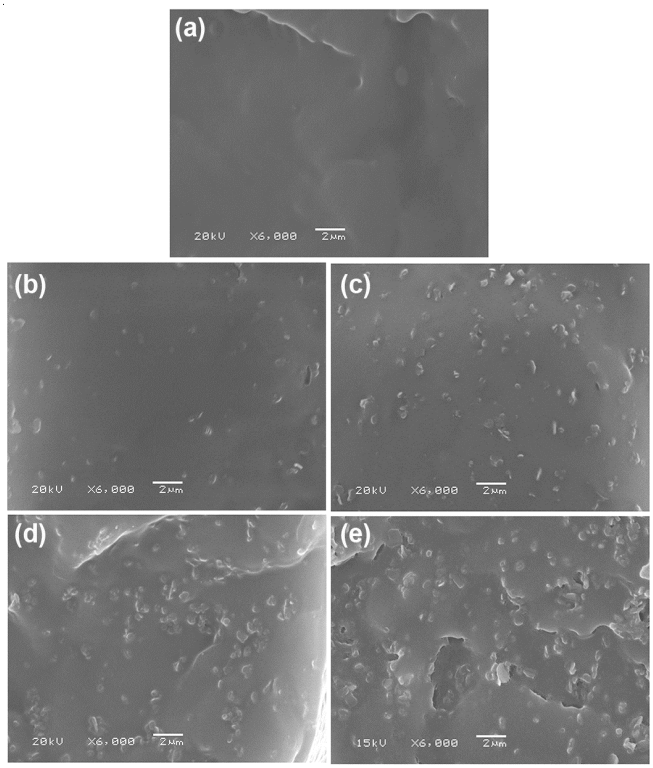

Fig. 7. SEM images of cryo-fractured cross-sections of (a) pure PLLA-PEG-PLLA film and PLLA-PEG-PLLA/BN films with BN contents of (b) 1, (c) 2, (d) 4 and (e) 6 wt%. (All bar scales = 2 μm)

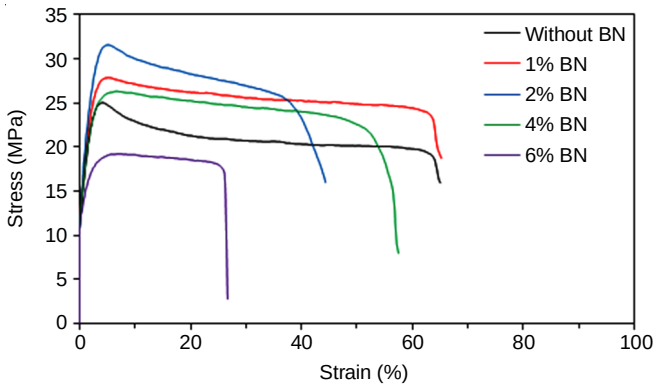

Fig. 8. Typical tensile curves of PLLA-PEG-PLLA/BN films with various BN contents

TABLE-5
AVERAGED TENSILE PROPERTIES OF PLLA-PEG-PLLA/BN FILMS

BN content (wt%)	Ultimate tensile stress (MPa)	Strain at break (%)	Young's modulus (MPa)
–	25.0 ± 2.4	76 ± 12	187 ± 21
1	27.8 ± 2.6	70 ± 11	229 ± 18
2	31.6 ± 1.8	64 ± 9	294 ± 28
4	26.3 ± 3.9	42 ± 15	207 ± 45
6	19.2 ± 4.1	24 ± 18	104 ± 37

increased while strain at break decreased when the boron nitride content increased up to 2 wt.%. These results indicated that the boron nitride particles induced a reinforcing effect on PLLA-PEG-PLLA films [15]. The composite films with 1 and 2 wt.% boron nitride showed a yield point indicating that they were flexible. The results suggested that interfacial adhesion on PLLA-PEG-PLLA/BN composites was strong enough to enhance stress transfer from the PLLA-PEG-PLLA matrix to the boron nitride particle surfaces to increase the tensile stress and Young's modulus of the composite films [15].

The ultimate tensile stress and Young's modulus of the composite films decreased when the boron nitride content was higher than 2 wt.%. This can be explained by aggregation of boron nitride particles in the PLLA-PEG-PLLA matrices as previously described from the SEM analysis. Aggregation of reinforced fillers reduced the mechanical properties of the polymer composites because decreased surface areas for stress transfer of fillers [2]. However, these PLLA-PEG-PLLA/BN composite films were still more flexible than the pure PLLA films (5-10% strain at break) [10].

Conclusion

A boron nitride reinforced flexible poly(L-lactide)-*b*-polyethylene glycol-*b*-poly(L-lactide) (PLLA-PEG-PLLA/BN) composite films have been successfully prepared by a casting method of PLLA-PEG-PLLA solution-boron nitride suspension in $CHCl_3$. The influence of boron nitride content on the thermal, morphological and mechanical properties of composite films was determined. The DSC study suggested that the addition of 1 and 2 wt.% boron nitride enhanced crystallization of PLLA blocks as observed by shifting of T_{cc} peaks to lower temperature, shifting of T_c peaks to higher temperature and reduction in $t_{1/2}$ values. The DSC-X_c values from DSC, 50%-T_d and $T_{d,max}$ values from TGA as well as XRD-X_c value from XRD of composite films increased as boron nitride content was increased up to 2 wt.% boron nitride. However, these values of composite films decreased significantly when the boron nitride content was higher than 2 wt.%. This was due to aggregation of boron nitride particles when the boron nitride contents were 4 and 6 wt.% as observed from SEM images of film cross-sections. The results of tensile testing showed that the highest ultimate tensile stress and Young's modulus of the composite films were obtained for 2 wt.% boron nitride. Further, a reduction in these tensile properties was found for 4 and 6 wt.% boron nitride. It can be concluded that the crystallizability, thermal stability and mechanical properties of PLLA-PEG-PLLA films can be improved by addition of 2 wt.% boron nitride. Thus, boron nitride can acts as both reinforcing filler and nucleating agent for PLLA-PEG-PLLA.

ACKNOWLEDGEMENTS

This work was financially supported by the Office of National Higher Education Science Research and Innovation Policy Council (NXPO), Thailand (grant no. PMU B05F6-30023). The Center of Excellence for Innovation in Chemistry (PERCH-CIC), Office of the Higher Education Commission, Ministry of Education, Thailand is also acknowledged.

CONFLICT OF INTEREST

The authors declare that there is no conflict of interests regarding the publication of this article.

REFERENCES

1. K. Hamad, M. Kaseem, M. Ayyoob, J. Joo and F. Deri, *Prog. Polym. Sci.*, **85**, 83 (2018); https://doi.org/10.1016/j.progpolymsci.2018.07.001
2. V.H. Sangeetha, H. Deka, T.O. Varghese and S.K. Nayak, *Polym. Compos.*, **39**, 81 (2018); https://doi.org/10.1002/pc.23906
3. G.-Z. Yin and X.-M. Yang, *J. Polym. Res.*, **27**, 38 (2020); https://doi.org/10.1007/s10965-020-2004-1
4. D. da Silva, M. Kaduri, M. Poley, O. Adir, N. Krinsky, J. Shainsky-Roitman and A. Schroeder, *Chem. Eng. J.*, **340**, 9 (2018); https://doi.org/10.1016/j.cej.2018.01.010
5. E. Balla, V. Daniilidis, G. Karlioti, T. Kalamas, M. Stefanidou, N.D. Bikiaris, A. Vlachopoulos, I. Koumentakou and D.N. Bikiaris, *Polymers*, **13**, 1822 (2021); https://doi.org/10.3390/polym13111822
6. E.M. Elmowafy, M. Tiboni and M.E. Soliman, *J. Pharm. Investig.*, **49**, 347 (2019); https://doi.org/10.1007/s40005-019-00439-x
7. B. Wang, Y. Jin, K. Kang, N. Yang, Y. Weng, Z. Huang and S. Men, *E-Polymers*, **20**, 39 (2020); https://doi.org/10.1515/epoly-2020-0005
8. H. Huang, Y.H. Zhang, L.S. Zhao, G.M. Luo and Y.H. Cai, *Mater. Plast.*, **57**, 28 (2020); https://doi.org/10.37358/MP.20.3.5377
9. X. Yun, X. Li, Y. Jin, W. Sun and T. Dong, *Polym. Sci. Ser. A*, **60**, 141 (2018); https://doi.org/10.1134/S0965545X18020141
10. Y. Baimark, W. Rungseesantivanon and N. Prakymoramas, *Mater. Des.*, **154**, 73 (2018); https://doi.org/10.1016/j.matdes.2018.05.028
11. Y. Baimark and Y. Srisuwan, *J. Elastomers Plast.*, **52**, 142 (2020); https://doi.org/10.1177/0095244319827993
12. A. Lotfi, H. Li, D.V. Dao and G. Prusty, *J. Thermoplast. Compos. Mater.*, **34**, 238 (2021); https://doi.org/10.1177/0892705719844546
13. S. Singha and M.S. Hedenqvist, *Polymers*, **12**, 1095 (2020); https://doi.org/10.3390/polym12051095
14. M. Pracella, M.M.U. Haque and D. Puglia, *Polymer*, **55**, 3720 (2014); https://doi.org/10.1016/j.polymer.2014.06.071
15. B. Bindhu, R. Renisha, L. Roberts and T.O. Varghese, *Polym. Test.*, **66**, 172 (2018); https://doi.org/10.1016/j.polymertesting.2018.01.018
16. F. Dumludag, M.Y. Yener, E. Basturk, S. Madakbas, V. Kahraman, M.A. Umer, U. Yahsi and C. Tav, *Polym. Bull.*, **76**, 4087 (2019); https://doi.org/10.1007/s00289-018-2560-2
17. D. Kong, D. Zhang, H. Guo, J. Zhao, Z. Wang, H. Hu, J. Xu and C. Fu, *Polymers*, **11**, 440 (2019); https://doi.org/10.3390/polym11030440
18. W. Kai, Y. He and Y. Inoue, *Polym. Int.*, **54**, 780 (2005); https://doi.org/10.1002/pi.1758
19. B. Ji, Y. Wu, P. Zhang and X. Zhao, *J. Polym. Res.*, **27**, 239 (2020); https://doi.org/10.1007/s10965-020-02189-z
20. F.A. Syamani, Y.D. Kurniawan and L. Suryanegara, *Asian J. Chem.*, **30**, 1435 (2018); https://doi.org/10.14233/ajchem.2018.21119
21. L. Li, Z.-Q. Cao, R.-Y. Bao, B.-H. Xie, M.-B. Yang and W. Yang, *Eur. Polym. J.*, **97**, 272 (2017); https://doi.org/10.1016/j.eurpolymj.2017.10.025
22. J. Jirum and Y. Baimark, *Asian J. Chem.*, **33**, 2135 (2021); https://doi.org/10.14233/ajchem.2021.23299
23. S. Saeidlou, M.A. Huneault, H. Li and C.B. Park, *Prog. Polym. Sci.*, **37**, 1657 (2012); https://doi.org/10.1016/j.progpolymsci.2012.07.005
24. K. Zhao, G. Liu, W. Cao, Z. Su, J. Zhao, J. Han, B. Dai, K. Cao and J. Zhu, *Polymer*, **206**, 122885 (2020); https://doi.org/10.1016/j.polymer.2020.122885
25. M. Öner, G. Kizil, G. Keskin, C. Pochat-Bohatier and M. Bechelany, *Nanomaterials*, **8**, 940 (2018); https://doi.org/10.3390/nano8110940